The active species and catalytic properties of CuO/CeO_2-TiO_2 catalysts for NO+CO reaction

JIANG XIAOYUAN*, LOU LIPING‡, DING GUANGHUI*, CHEN YINGXU‡, ZHENG XIAOMING*
*Institute of Catalysis and ‡Department of Environmental Science, Zhejiang University, Hangzhou, 310028, People's Republic of China
E-mail: xyjiang@mail.hz.zj.cn

Nitrogen oxides (NO_x) are one of the major air pollutants in modern cities, largely due to the exhaust of automobiles. The elimination of NO_x by catalysts has received high attention as NO_x pollution intensifies. Since Iwamoto *et al.* reported selective reduction of NO_x with hydrocarbon in an oxygen-enriched atmosphere by Cu-ZSM5 and other ionic-exchanged catalysts [1, 2], many catalysts have been studied and one of them is CuO/TiO_2 catalyst [3–5]. This catalyst has high activity in the oxidation of CO and hydrocarbon [6, 7] and the selective reduction of NO [8–11]. It also has an excellent prospect in the purification of stack gases which contain NO, CO and other organic waste gases [12]. The studies also showed that the nanometer form of Cu^{2+} ion was more active than the bulk CuO in both NO reduction and selective reduction of NO_x with NH_3 by catalysts. The ionic state of Cu^{2+} on CuO/TiO_2 catalyst was detected by the methods of ESR, XRD and UV-VIS, and the stability of Cu ion was related to the interaction with O^- ion in the TiO_2 crystal lattice [13–15]. If Cu ion was adsorbed on the surface of anatase (TiO_2), two Cu^{2+} species would coordinate with two kinds of Lewis acid sites in different forms. The TPR analysis found that two Cu^{2+} species with different reduction abilities existed on the surface of anatase (TiO_2) [16]. The high-temperature reduction peak was attributed to the reduction of bulk CuO, but the low-temperature reduction peak was derived from the interaction of Cu^{2+} and the carrier that caused the reduction of CuO. Wollner *et al.* [17] reported that CuO/TiO_2 and Cu-ZSM5 had similar activity in the reaction of NO+CO, and the removing rate reached 95% at 200 °C. In the CO and organic oxidation reaction, CuO had much higher activity than MoO_X, FeO_X and CoO_X if TiO_2 was used as a carrier [6, 7]. CuO/TiO_2 activity at low temperature was even higher than Pt/γ-Al_2O_3 and was largely enhanced by the addition of CeO_2. This was because CeO_2 had a special function of oxygen storage and increased the dispersion of the active component of catalyst on the carrier and the thermal stability of the carrier [18]. In this study, TiO_2 and CeO_2-TiO_2 were prepared by the sol-gel method, and the effects of CuO loading on structures and catalytic activities in NO+CO reaction were examined by means of BET, TPR, XRD, XPS and NO-TPD.

TiO_2 carrier was prepared using the solution-gelation method [19]. Solution A was a mixture of HCl, H_2O and half of ethanol, and Solution B was obtained after $Ti(OC_4H_9)_4$ was dissolved in the other half of ethanol. Solution A was added to Solution B, and the mixture was left for several days. The resulting gel of $HCl:H_2O$:ethanol:$Ti(OC_4H_9)_4$ = 1:15:1:0.3 was air-dried at 50 °C for 12 h and then calcined at 500 °C for 2 h.

Using TiO_2 as a carrier, the CuO/TiO_2 and CuO/CeO_2-TiO_2 catalysts were prepared by the impregnation method using $Cu(NO_3)_2$ and $Ce(NO_3)_3$ aqueous solutions at desired concentrations. The catalysts were dried at 120 °C for 12 h and then calcined in an air stream at 500 °C for 2 h, and denoted as w%CuO/TiO_2 and w%CuO/w′%CeO_2-TiO_2, where w and w′ were the amount of CuO and CeO_2 loadings, respectively.

Catalytic activity was determined under the steady state in a fixed-bed quartz reactor (6 mm). The particle size of catalysts was 20–40 mesh, and 120 mg of the catalysts were used. The reaction gas (i.e., feed steam) consisted of a fixed composition of 6.0%NO, 6.0%CO and 88%He (v/v) as a dilute. The catalysts were pretreated in NO+CO reaction stream at 50 °C for 0.5 h. After having cooled to room temperature, they were allowed to react with the mixed gas. The reactions were operated at different temperatures with a space velocity of 5000 h^{-1}. Two columns and thermal conduction detectors were used for analyzing the catalytic activity. Column A was packed with 13X molecular sieve for separating N_2, NO and CO, and Column B was packed with Paropak Q for separating N_2O and CO_2.

The BET surface area of catalysts was determined by N_2 adsorption at 77 K using a Coulter OMNISORP-100 instrument.

H_2-temperature programmed reduction (TPR) was done by gas chromatography (GC) using a thermal conductivity detector. Samples of 5–10 mg were activated in an O_2 stream at 500 °C for 0.5 h. After it was cooled to 30 °C, H_2-TPR was conducted.

X-ray diffraction (XRD) data were obtained at 25 °C using a horizontal Rigaku B/Max 111B powder diffractometer with Cu K_α radiation and a power of 40 × 30 mA.

X-ray photoelectron spectra (XPS) were recorded by PHI-550 Spectrometer with Al K_α radiation of 1486.6 eV. The calibration of the spectrometer energy scale was performed using gold (Au $4f_{7/2}$ = 83.8 eV). The C1s line at 284.6 eV was used as an internal standard for correction of binding energies. The accuracy of energy values was 0.3 eV.

0022–2461

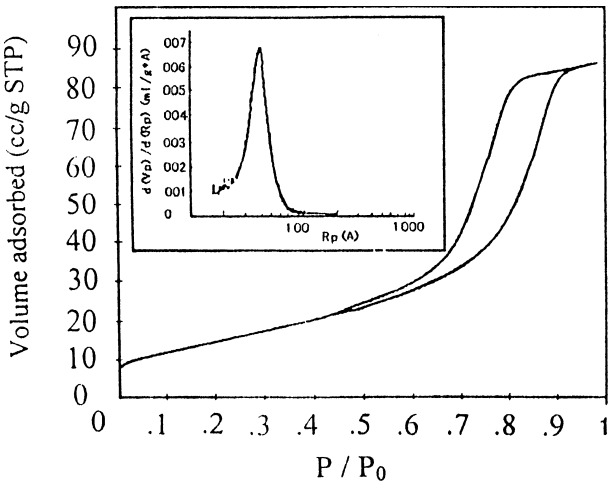

Figure 1 Adsorption-desorption isotherms and pore size distribution of TiO_2.

To measure NO-temperature programmed desorption (TPD), 250 mg of fresh catalysts were loaded onto a quartz reactor ($\Phi = 5$ mm) and reduced in H_2 atmosphere at 500 °C for 1.0 h. The catalysts were then heated in He at 600 °C for 1.0 h, cooled to 40 °C in a flow of He and exposed to a 10%NO–He mixture gas. Excessive NO was removed, and the catalysts were kept in He flow until no significant amount of adsorbates could be detected. The catalysts were then ramped at 600 °C at a linear heating rate of 20 °C min^{-1} in He flow. The effluent gases were analysed with a mass spectrometer.

The structural properties of TiO_2 were examined by measuring its N_2 adsorption and desorption, an important method of revealing multi-porous solid substances. As shown in Fig. 1, the TiO_2 adsortion-desorption isotherms were of Type IV, a typical mesoporous substance, and its pore size distribution proved the existence of mesopores but not regular pores. In contrast, the pore size distribution of TiO_2 was microporous, slightly toward mesoporous, and had a specific surface area of 54.938 m^2/g and total porous volume of 0.1518 ml/g.

The X-ray diffraction analysis found that TiO_2 consisted of a mixture of anatase and rutile phases. The catalytic activity in NO+CO reaction at different CuO loading on TiO_2 is shown in Fig. 2a–d. At CuO loading of $\leq$3.0% (w/w), the catalytic activity in NO+CO reaction was quite low. The activity largely increased at 6 % CuO loading and reached the maximum at 12.0 % CuO loading, and further increase in CuO loading caused a decrease in catalytic activity. However, after TiO_2 was modified with 5.0 % and 10.0 % CeO_2, the CuO/CeO_2-TiO_2 activity was much higher than non-CeO_2-modification, especially for the CuO/TiO_2 catalyst with low CuO loading (e.g., $\leq$3.0%). At 450 °C, NO conversion was close to zero by 3.0 % CuO/TiO_2 but increased to 85% by 3.0 % CuO/5.0 % CeO_2-TiO_2 and reached 95% by 3.0 % CuO/10.0 % CeO_2-TiO_2. NO conversion was complete (100%) under the following conditions: 12.0 % CuO/TiO_2 at 400 °C, 12.0 % CuO/5.0 % CeO_2-TiO_2 at 350 °C, 12.0 % CuO/10.0 % CeO_2-TiO_2 at 300 °C. The catalytic activity in NO+CO reaction may be related to, 1) the dispersed Cu species on TiO_2 with a best CuO loading amount, 2) the interaction between redox couple (Ce^{4+}/Ce^{3+}) of CeO_2 with CuO and TiO_2.

As shown in Table I, 12 % CuO/TiO_2 catalyst had smaller CuO crystalline size. In addition, the catalyst had larger micro-strain value than 3 % CuO/TiO_2 and 18 % CuO/TiO_2 catalysts but smaller micro-strain value than 12 % CuO/5 % CeO_2-TiO_2 and 18 % CuO/5 % CeO_2-TiO_2 catalysts. The catalytic

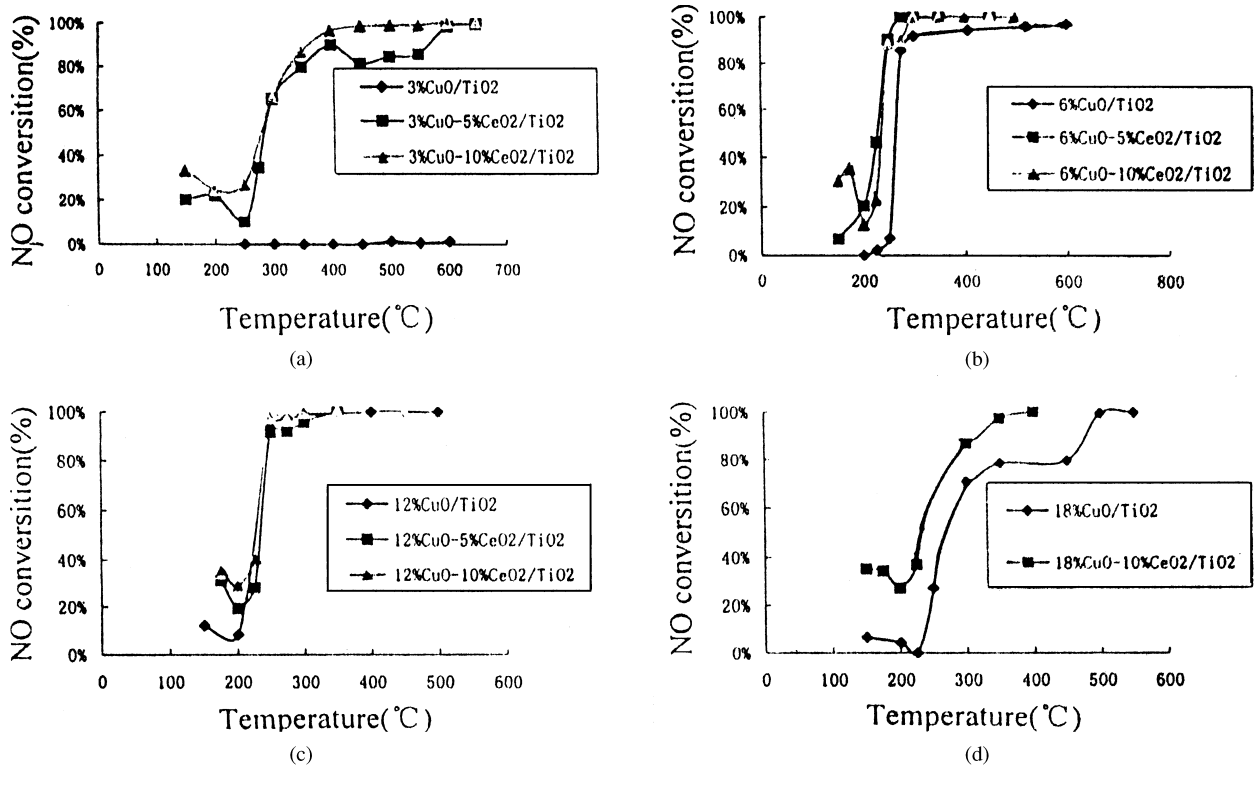

Figure 2 The activity of CuO/TiO_2 and CuO/CeO_2-TiO_2 with different CuO loading in NO+CO reaction.

TABLE I Micro-structure analysis results of CuO/TiO_2 and CuO/CeO_2-TiO_2

Catalysts	CuO crystalline size (nm)	Micro-strain	Anatase crystalline size (nm)	Rutile crystalline size (nm)	Micro-strain	Cell parameters (nm) (a)	Cell parameters (nm) (c)
3 % CuO/TiO_2	32.75	2.20×10^{-4}		89.65	1.0×10^{-4}	4.6039(68)	2.9638(13)
12 % CuO/TiO_2	28.08	3.19×10^{-4}		85.20	6.1×10^{-4}	4.5910(3)	2.9518(2)
18 % CuO/TiO_2	35.50	1.30×10^{-4}		92.04	1.0×10^{-4}	4.9516(5)	2.9592(3)
12 % CuO/5 % CeO_2-TiO_2	26.83	4.96×10^{-3}	60.58	63.28	2.9×10^{-4}	4.5945(13)	2.9614(7)
12 % CuO/10 % CeO_2-TiO_2	25.8	2.94×10^{-3}	46.84	46.84	3.0×10^{-3}	4.5936(30)	2.9541(21)
12 % CuO/5 % CeO_2-TiO_2	26.37	3.63×10^{-3}	51.33	59.59	2.8×10^{-4}	405961(34)	2.9607(24)

activity in NO+CO reaction was related to the crystalline size and the micro-strain value. The smaller the crystalline size and the larger the micro-strain value were, the higher was the catalytic activity. Interestingly, the crystalline size and micro-strain of the carrier were not affected by the amount of CuO loading, whereas at a given CuO amount, the smaller the crystalline size of the carrier and active component, the larger was the micro-strain value. Among the CuO/TiO_2 catalysts, both TiO_2 and CuO in 12 % CuO/TiO_2 had the smallest crystalline size and the largest micro-strain, indicating that although the carrier had a stronger effect than the active component, the latter could in turn affect the function of the former. This may explain that active component CuO with different carriers would differ largely in the catalytic activity. Small crystalline size and large micro-strain are indispensable for CuO to have high activity because such CuO surface has higher energy.

Fig. 3 shows the TPR profiles of pure CuO, TiO_2 and TiO_2 with different CuO loading (3.0–18.0%). Pure CuO had a large and sharp crystal phase reduction peak at 392 °C, while pure TiO_2 had a rather flat reduction peak at a higher temperature (about 650 °C), suggesting

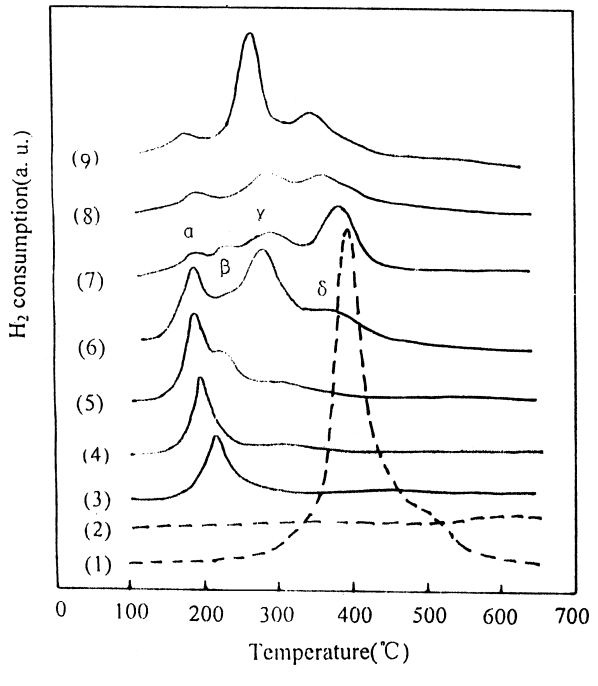

Figure 3 TPR profiles of CuO/TiO_2 and CuO/CeO_2-TiO_2 catalysts. (1) CuO, (2) TiO_2, (3) 1 % CuO/TiO_2, (4) 3 % CuO/TiO_2, (5) 6 % CuO/TiO_2, (6) 12 % CuO/TiO_2, (7) 12 % CuO/5 % CeO_2-TiO_2, (8) 6 % CuO/10 % CeO_2-TiO_2, (9) 12 % CuO/10 % CeO_2-TiO_2.

that CuO reduction was easier than TiO_2 reduction. After TiO_2 and CeO_2 formed the composite oxide, the interaction of TiO_2 and CeO_2 increased the reduction of TiO_2. When the CuO loading was 3.0 wt%, there was only one reduction peak in the whole TPR process (Fig. 3, Line 4). At 6.0 wt% CuO loading, a γ peak of CuO crystal phase was observed. At 12 wt% CuO loading, there were four reduction peaks in different sizes (namely α, β, γ and δ peaks) at peak temperatures of 180, 240, 290 and 380 °C respectively. The α peak temperature of 12 wt%CuO/TiO_2 was lower than that of other catalysts (Line 6). When CuO was loaded on 5.0 % CeO_2-TiO_2 and 10.0 % CeO_2-TiO_2 (Lines 7 to 9), there were still four reduction peaks (α, β, γ and δ), but these reduction peaks were not obvious. The peak temperature of CuO reduction in 10.0 % CeO_2-TiO_2 occurred slightly earlier than that in 5.0 % CeO_2-TiO_2.

The CuO/TiO_2 catalyst is a complex catalytic system. According to Larsson *et al.* [6, 7], the forms of Cu species in Cu3-Ti, Cu12-Ti and Cu-Ce-Ti were different. The reduction peak of Cu3-Ti was at 200 °C, representing the reduction of monomeric Cu species (mainly Cu^+). By comparison, the reduction peak of Cu12-Ti was at 180 °C, representing the reduction of polymeric Cu species (mainly Cu^{2+}). While monomeric Cu species in Cu3-Ti and Cu12-Ti would convert to polymeric Cu species when CeO_2 content increased, the polymeric Cu species had higher activity than the monomeric Cu species. Komova *et al.* [20] found that the form of Cu species in Cu—Ti—O was determined by the structure of CuO on the surface of TiO_2, the amount of CuO loading and the preparation method of Cu—Ti—O. When the CuO loading was low, Cu^{2+} readily interacted with oxygen atom (O), which was poorly coordinated in the anatase crystal lattice. When the CuO loading was high, surface-stable Cu^{2+} and chain oxidation cluster readily formed as the active center. Cordoba *et al.* [21] used the characterizing techniques of ESR, TPR, XPS and classified the Cu species on the surface of TiO_2 into three states: Cu^{2+} in the TiO_2 network (namely, —Cu—O—Ti—O—), isolated CuO and highly-dispersed polymeric CuO. The Cu^{2+} in the TiO_2 network was probably the surface stable Cu^{2+} and chain oxidation cluster, as suggested by Komova [20].

Based on the TPR results above, we suggest that α and β peaks were the reduction peaks of highly-dispersed Cu species, γ peak was the reduction peak of CuO crystal phase in different crystalline size [7, 21], while δ peak was the reduction peak of TiO_2 catalyzed

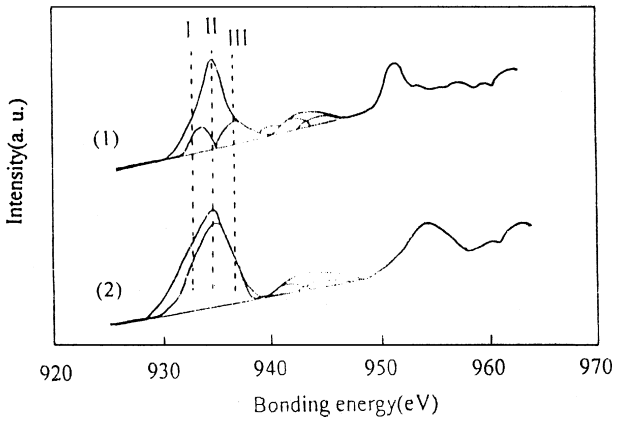

Figure 4 Comparison of bonding energy of $Cu2p_{3/2}$ of 12 % CuO/TiO_2 and 12 % CuO/10 % CeO_2-TiO_2.

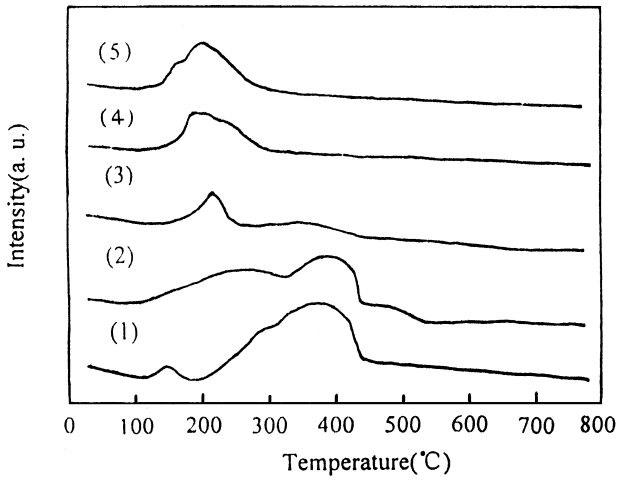

Figure 5 Detected NO signal during NO-TPD processing. (1) TiO_2, (2) CeO_2-TiO_2, (3) 6 % CuO/TiO_2, (4) 6 % CuO/5 % CeO_2-TiO_2, (5) 12 % CuO/5 % CeO_2-TiO_2.

by CuO [15, 21]. The interaction between CuO, CeO_2 and TiO_2, and CeO_2 and TiO_2 increased the activity of CuO reduction [6].

There were three forms of Cu species in 12 % CuO/TiO_2 with the bonding energies of 932.59, 934.62 and 937.04 eV respectively (Fig. 4). The 934.62 eV peak was the main one and accounted for 66.1% (Table II). In accordance with standard bonding energy value [17], we presume that the 932.59 eV peak was Cu^+, while the 934.62 and 937.04 eV peaks were CuO and —Cu—O—Ti—O—, denoted as Cu^{2+}(I) and Cu^{2+}(II), respectively. The addition of CeO_2 caused the disappearance of Cu^{2+}(II) and the increment of Cu^{2+}(I) and Cu^+, the main active components in the NO+CO reaction [22, 23]. As a result, the addition of CeO_2 enhanced the activity of CuO/TiO_2 catalyst. In addition, the atom ratio of Cu/Ce exceeded that of Cu/Ti in the 12 % CuO/10 % CeO_2-TiO_2 catalyst (Table II), indicating that Cu species were predominantly dispersed on the surface of CeO_2.

At low CuO concentration, Cu^{2+} first coordinated with the low-coordinated oxygen atom (O) in the anatase lattice to form a chain structure, i.e., —Cu—O—Ti—O— structure [20]. The bonding energy of the species coordinated with the low-coordinated O atom was quite high. For example, Cu^{2+}(II) showed higher bonding energy than Cu^{2+}(I). We presume that the decrease of CuO bonding energy in 12 % CuO/10 % CeO_2-TiO_2 was due to the earlier loading of CeO_2 than CuO. Therefore, CeO_2 first combined with low-coordinated oxygen atom (O), and the later-loaded CuO only formed Cu^{2+}(I) using the species as the core. The bonding energy of Ce3d($3d^9 4f^2(O2p^4)$) in 12 % CuO/10 % CeO_2-TiO_2 was 883.34 eV, higher than that of single CeO_2(882.3 eV), which proved the above hypothesis.

NO-TPD experiment of carrier and catalyst was conducted to further examine the mechanism of NO+CO reaction. After NO was adsorbed by the surface of carriers (TiO_2 and CeO_2-TiO_2) and catalysts (CuO/TiO_2 and CuO/CeO_2-TiO_2), NO and N_2O were detected by mass spectrometer tracking. Figs 5 and 6 show four desorption species (NO, $m/e = 30$; N_2O, $m/e = 44$; O_2, $m/e = 32$ and NO_2, $m/e = 46$) after TiO_2 adsorbed NO and dissociation reaction occurred. The NO desorption process had two small peaks and a big peak, i.e., three NO adsorbing centres with different intensities on the TiO_2 surface. The two small peaks occurred at 100 and 280 °C respectively, and the big peak at 385 °C. After CeO_2-TiO_2 adsorbed NO, the thermal desorption process also had three peaks, but the first two were big peaks and the third was a small peak. Although

TABLE II Bonding energy and atomic ratio of 12 % CuO/TiO_2 and 12 % CuO/10 % CeO_2-TiO_2

		12 % CuO/TiO_2	12 % CuO/10 % CeO_2-TiO_2
Ce3d($3d^9 4f^2(O2p^4)$)	B.E. (eV)	–	883.34
$Ti2P_{3/2}$	B.E. (eV)	458.3	458.9
O1sLattice	B.E. (eV)	529.6	530.1
Cu^+	B.E. (eV)	932.59	932.5
	Proportion (%)[a]	17.5	19.1
Cu^{2+}(I)	B.E. (eV)	934.62	934.65
	Proportion (%)[a]	66.1	80.9
Cu^{2+}(II)	B.E. (eV)	937.04	–
	Proportion (%)[a]	16.4	–
Cu/(Ti+Ce)	Atomic ratio	–	0.366
Cu/Ce	Atomic ratio	–	3.112
Cu/Ti	Atomic ratio	0.39	0.42
Ce^{3+} (%)	Proportion (%)[b]	–	0.272

[a]Percentage of total Cu species.
[b]Percentage of total Ce species.

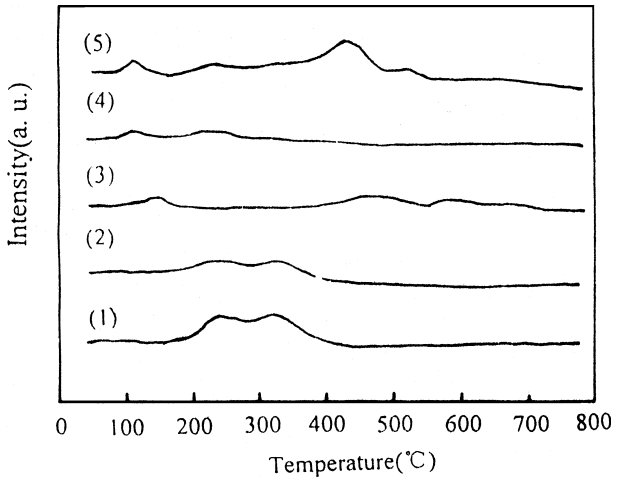

Figure 6 Detected N_2O signal during NO-TPD processing. (1) TiO_2, (2) CeO_2-TiO_2, (3) 6 % CuO/TiO_2, (4) 6 % CuO/5 % CeO_2-TiO_2, (5) 12 % CuO/5 % CeO_2-TiO_2.

NO desorption on the carrier (TiO_2 and CeO_2-TiO_2) was larger than that on the catalyst, NO dissociation activity was low on all the adsorbing sites and only a small amount of NO dissociated at 200 °C (Fig. 6). In addition, the peak temperature of NO desorption on the catalyst was lower than that on the carrier (Fig. 5, Lines 3, 4, 5), and the NO dissociation temperature occurred earlier and the NO desorption was larger on CuO/CeO_2-TiO_2 than those on CuO/TiO_2 (Fig. 6). The findings suggest that the temperature of N_2O formation (i.e., NO dissociation temperature) was correlated with the activities of catalysts. Namely, the rate of NO+CO reaction was determined by the NO dissociation on the catalyst surface.

Acknowledgment

This work was financially supported by the Environmental Protection Bureau of Hangzhou (200220).

References

1. M. IWAMOTO, H. YAHIRO, Y. MINE and S. KAGAWA, *Chem. Lett.* (1989) 213.
2. M. IWAMOTO, H. YAHIRO, T. TORIKAI, T. YOSHROKA and N. MIZUNO, *ibid.* (1990) 1967.
3. S. P. MARIA, R. M. VALMOR, A. P. PEDRO and O. F. ARIOVALDO, *J. Phys. Chem.* B **105** (2001) 10515.
4. M. TATSUO, *Appl. Catal. B: Environm.* **16** (1998) 155.
5. F. BOCCUZZI, E. GUGLIELMINOTTI, G. MARTRA and G. CERRATO, *J. Catal.* **146** (1994) 449.
6. P. LARSSON, A. ANDERSSON, L. WALLENBERG and B. SVENSSON, *ibid.* **163** (1996) 279.
7. P. LARSSON and A. ANDERSSON, *ibid.* **179** (1998) 72.
8. O. V. KOMOVA, A. V. SIMAKOV and L. T. TZYKOZA, *React. Kinet. Catal. Lett.* **54** (1995) 361.
9. G. CENTI, C. NIGRO, S. PERATHONER and G. STELLA, *Catal. Today* **17** (1993) 159.
10. G. CENTI, S. PERATHONER, B. KARTHEUSER and B. HODNETT, *ibid.* **17** (1993) 103.
11. G. CENTI, S. PERATHONER and B. KARTHEUSER, *Appl. Catal.* **1** (1992) 129.
12. O. V. KOMOVA, A. V. SIMAKOV and L. T. TZYKOZA, *React. Kinet. Catal. Lett.* **54** (1995) 371.
13. M. M. KANTCHEVA, K. HAJIIVANOV and A. A. DAVYDOV, *Appl. Surf. Sci.* **55** (1992) 49.
14. K. HAJIIVANOV, D. KLISSURSKI, M. M. KANTCHEVA and A. DAVYDOV, *J. Chem. Soc. Faraday Trans.* **87**(6) (1991) 907.
15. B. XU, L. DONG and Y. CHEN, *ibid.* **94**(13) (1998) 1905.
16. M. ARCO, A. CABALLERO, P. MALET and V. RIVES, *J. Catal.* **113** (1988) 120.
17. A. WALLNER and F. LANGE, *Appl. Catal. A: General* **94** (1993) 181.
18. X. Y. JIANG, G. L. LU, R. X. ZHOU and X. M. ZHENG, *Appl. Surf. Sci.* **173** (2001) 208.
19. Y. X. CHEN, L. P. LOU, X. Y. JIANG and X. M. ZHENG, *Indian J. Chem.* A **43** (2003) 460.
20. O. V. KOMOVA, A. V. SIMAKOV and V. A. ROGOV, *J. Mol. Catal. A: Chem.* **161** (2000) 191.
21. G. CORDOBA, M. VINIEGRA and J. FIERRO, *J. Sol. Chem.* **138** (1998) 1.
22. C. DROUET, P. ALPHONSE and A. ROUSSET, *Appl. Catal.* B **33** (2001) 35.
23. Y. H. HU, L. DONG, M. M. SHEN, D. LIU and J. WANG, *ibid.* **31** (2001) 61.

Received 18 December 2003
and accepted 18 March 2004